Research on Engineering Structures & Materials
www.jresm.org
Research Group

Research Article

Evaluation of self-compacting concrete for concrete repair applications

Hachemi Benaddi[1,a], Billel Rebai[1,b], Tidjani Messas[1], Mohamed Salhi[2,c]

[1]*Civil Engineering Department, Abbes Laghrour University, BP. 1252, Khenchela 4004, Algeria*
[2]*Civil Engineering Department, University of Relizane, Algeria*

Article Info

Article history:

Received 23 April 2024
Accepted 25 June 2024

Keywords:

Self-compacting concrete;
Concrete repairs;
Mechanical properties;
Bond strength;
Mineral additives;
Limestone fillers;
Blast furnace slag;
Silica fume;
Adhesion tests

Abstract

This study investigates the suitability of utilizing Self-Compacting Concrete (SCC) as a repair material for concrete structures. Various SCC mixtures were formulated with different compositions, including 100% cement, 30% limestone fillers, 40% blast furnace slag, and 10% silica fume. The fresh properties, such as fluidity, deformability, and stability, were evaluated to optimize the SCC mixtures for repair applications. The mechanical properties, including compressive strength, tensile strength, and elastic modulus, were assessed and compared to vibrated ordinary concrete (VOC). Additionally, the bond strength between the SCC repair material and the existing concrete substrate was investigated using simulated repair specimens subjected to indirect tensile bond and splitting tensile bond tests. The results demonstrated the superior mechanical performance of SCC compared to VOC, with higher compressive and tensile strengths. Furthermore, the incorporation of mineral additives, such as limestone fillers, slag, and silica fume, enhanced the mechanical properties and bond strength of the SCC mixtures. The study highlights the potential advantages of using SCC over VOC for concrete repair applications, offering improved mechanical performance and adhesion characteristics.

© 2024 MIM Research Group. All rights reserved.

1. Introduction

Achieving a robust and durable bond between repair materials and existing concrete substrates is a pivotal challenge in concrete repair and rehabilitation projects. The field of civil engineering has seen extensive research efforts aimed at optimizing various aspects of the concrete repair process, such as bonding durability [1], thin repairs [2], experimental methodologies and modeling techniques [3, 27], and hydraulic and mechanical interactions [4]. Specialized tests have been developed to assess substrate cohesion [5] and quantify adhesion [6, 28], emphasizing the importance of proper surface preparation [7].

Compatibility between repair materials and the existing concrete matrix is crucial to prevent future issues like cracking and debonding [8]. Selecting appropriate repair materials depends on factors such as the extent of damage, prevailing load conditions, and environmental influences [9]. For reinforced concrete structures, repair interventions must restore structural integrity and ensure long-term durability [10]. A strong repair-substrate bond involves both mechanical interlocking and chemical bonding mechanisms between the old and new concrete layers [11]. Additionally, meticulous curing practices are essential to achieve the desired strength and performance characteristics [12].

*Corresponding author: billel.rebai@univ-khenchela.dz
[a]orcid.org/0000-0002-2792-6159; [b]orcid.org/0000-0003-3739-2784; [c]orcid.org/0000-0001-9285-9442
DOI: http://dx.doi.org/10.17515/resm2024.255st0423rs

The adhesion between repair materials and substrates involves a complex interplay of chemical bonding and mechanical interlocking mechanisms [6]. Various solutions, including dry/wet shotcrete, formwork, and self-compacting concrete (SCC), offer promising avenues for enhancing adhesion in repair and reinforcement scenarios. Adhesion assessment typically involves subjecting specimens to tension, flexion, and/or shear stresses [13, 14]. Bond tests are crucial for quantifying the adhesion of repair systems to concrete substrates, employing direct or indirect tensile stress generation methodologies [29].

This study investigates the potential of utilizing Self-Compacting Concrete (SCC) as a repair material for concrete structures. The research focuses on formulating and characterizing various SCC mixtures with compositions including 100% cement, 30% limestone fillers, 40% blast furnace slag, and 10% silica fume. The fresh and hardened properties of these SCC mixtures are evaluated and compared to vibrated ordinary concrete (VOC). Additionally, the study assesses the bond strength between the SCC repair material and the existing concrete substrate using simulated repair specimens.

Recent research has demonstrated the suitability of SCC for concrete repair applications due to its excellent fluidity, stability, and bond strength [15, 30]. Studies have explored different SCC mix designs for repair overlays, incorporating steel fibers for enhanced strength [16]. The development of self-healing concrete technology offers a solution to micro-cracks in concrete structures, with Bacillus Subtilis bacteria proving effective in promoting self-recovery of cracks [17]. Evaluating the long-term durability of self-healing concrete is crucial, focusing on resistance to fatigue, creep, and corrosion, alongside mechanical properties assessments [18].

Furthermore, recycled self-compacting concrete, which utilizes recycled aggregates, presents challenges such as reduced flowability and strength but offers benefits like internal curing effects to reduce shrinkage [21]. Lightweight self-compacting concrete has also shown promise in civil engineering applications, achieving densities below 1000 kg/m^3 while maintaining strength and durability, making it a viable option for repair work [24]. The use of self-healing technology with SCC has been explored to control moisture ingress and enhance durability in repair mortars, demonstrating a reduction in sorptivity coefficients and improved autonomous healing efficiency, beneficial for concrete repair applications in terms of longevity and performance [25].

Overall, the combination of SCC's properties, lightweight characteristics, and self-healing capabilities makes it a compelling choice for concrete repair applications, offering enhanced durability and longevity [26]. This study aims to contribute to the existing body of knowledge by evaluating the performance of SCC as a repair material and investigating its bond strength with existing concrete substrates.

2. Materials Used

2.1. Cement

The cement used in all mixtures is CEM I/42.5 grade from the GIGA group of the Ain-Touta cement plant, located in Algeria. The physical characteristics of this cement include an absolute density of 3.1, an apparent density of 1.13, and a Blaine specific surface of 3917 cm2/g. The normal consistency of the cement is 27.2% H2O, with a start time of 2 hours and 12 minutes and an end time of 3 hours and 8 minutes. The hot expansion of the cement is 0.50 mm.

2.2. Sand

The sand used in this study is a local silica sand with a granular class of 0/5 mm, extracted from Oued Ittel, located 85 km south of Biskra, Algeria. This approach is supported by several studies, such as those conducted by de Larrard (1999) and Fennis et al. (2009) [30], which demonstrate the improved mechanical properties and durability of concrete when using gap-graded aggregates. The sand's properties, including absolute density, apparent density, fineness modulus, and visual sand equivalent, were determined according to the standard testing methods [31]. The values obtained for the sand's absolute density, apparent density, fineness modulus, and visual sand equivalent were 2.56, 1.54, 2.54, and 78.32, respectively.

The measurements were performed as follows:

- Absolute density: The sand sample was oven-dried at 105°C for 24 hours, cooled to room temperature, and then immersed in water for 24 hours. The saturated surface-dry (SSD) condition was achieved by removing the surface moisture using a dry cloth. The SSD sand was weighed in air and water, and the absolute density was calculated using the formula specified in ASTM C128.
- Apparent density: The sand sample was oven-dried at 105°C for 24 hours and cooled to room temperature. The dry sand was placed in a cylindrical container of known volume, and the mass of the sand was measured. The apparent density was calculated by dividing the mass of the sand by the volume of the container.
- Fineness modulus: The sand sample was oven-dried at 105°C for 24 hours and cooled to room temperature. The dry sand was sieved through a series of standard sieves (4.75 mm, 2.36 mm, 1.18 mm, 0.60 mm, 0.30 mm, and 0.15 mm), and the cumulative percentage retained on each sieve was calculated. The fineness modulus was determined by adding the cumulative percentages retained on each sieve and dividing the sum by 100.
- Visual sand equivalent: The sand sample was placed in a graduated cylinder with a flocculating solution, agitated, and allowed to settle for 20 minutes. The height of the sand and clay layers was measured, and the sand equivalent value was calculated by dividing the height of the sand layer by the total height of the sand and clay layers, expressed as a percentage.

The values obtained for the sand's absolute density, apparent density, fineness modulus, and visual sand equivalent were 2.56, 1.54, 2.54, and 78.32, respectively.

2.3. Gravel

The physical properties of the crushed limestone gravel from the Ain-Touta deposit in the Batna province of Algeria were determined according to relevant testing standards. The absolute density and absorption coefficient were measured as per ASTM C127 [31], while the apparent density and porosity were determined using ASTM C29/C29M [31]. The Los Angeles coefficient, which assesses the resistance to abrasion and impact, was evaluated following ASTM C131/C131M [31].

The use of gap-graded gravel sizes (7/15 and 15/25) in concrete mixture design is a common practice that offers several advantages. The combination of smaller and larger gravel sizes helps to optimize the packing density by minimizing void spaces between particles, resulting in a denser and more compact concrete matrix [30]. The smaller gravel size (7/15) enhances the workability and filling ability of self-compacting concrete (SCC) by reducing interparticle friction and facilitating mixture movement [32]. On the other hand, the larger gravel size (15/25) is typically used in conventional vibrated concrete to improve interlocking and load transfer between particles, leading to higher strength and stability [33].

The physical characteristics of the gravel were determined for two size ranges: Gravel 15/25 and Gravel 7/15. The absolute density values were found to be 2.62 and 2.61, respectively, while the apparent density values were 1.255 and 1.283. The absorption coefficient values were 0.64 and 0.60, and the porosity values were 0.96 and 0.56. The Los Angeles coefficient was found to be 26 for both gravel sizes, indicating a satisfactory level of durability [34].

2.4. Limestone Fillers

The crushed limestone rock used in this study is sourced from the quarries of Ain-Touta, Algeria. The laboratory analysis of the limestone filler revealed an absolute density of 2.76, an apparent density of 1.09, and a specific surface area of 3070 cm2/g. The absolute density was determined using the pycnometer method, as described in ASTM C128 [31], which involves measuring the displacement of a liquid (usually water) by a known mass of the material. The apparent density was measured using the ASTM C29/C29M standard [31], which involves filling a container of known volume with the material and determining its mass. The specific surface area was determined using the Blaine air permeability method, as outlined in ASTM C204 [31], which measures the time required for a fixed volume of air to pass through a compacted bed of the material.

The incorporation of limestone fillers in self-compacting concrete (SCC) mixtures has been shown to improve various properties of the concrete. Limestone fillers contribute to the workability and cohesiveness of the mixture by increasing the paste volume and improving the particle packing density [34]. The increased packing density results in a reduction of the water demand for a given workability [35]. Additionally, the fine limestone particles act as nucleation sites for the formation of hydration products, leading to an enhancement in the mechanical properties of the concrete [36].

2.5. Blast Furnace Slag

It is a granulated and ground blast furnace slag product from the El-Hadjar steel complex in Annaba, Eastern Algeria. Its physical characteristics are as follows: absolute density = 2.73, apparent density = 1.08, and specific surface area = 3000 cm2/g. The absolute density was determined using the pycnometer method, as described in ASTM C188 [31], while the apparent density was measured using the ASTM C29/C29M standard [31]. The specific surface area was determined using the Blaine air permeability method, as outlined in ASTM C204 [31]. The chemical composition of the blast furnace slag, with its respective proportions in percentage, is as follows: SiO2 (40.8%), CaO (43.0%), MgO (6.4%), Al2O3 (5.2%), MnO (3.0%), S (0.8%), and Fe2O3 (0.5%).

The use of blast furnace slag as a partial replacement for cement in self-compacting concrete (SCC) mixtures can improve various properties of the concrete. Blast furnace slag exhibits pozzolanic properties, reacting with calcium hydroxide produced during cement hydration to form additional calcium silicate hydrates, contributing to strength development over time [38]. The incorporation of slag in SCC mixtures can enhance the workability and cohesiveness of the mixture, as the slag particles act as a filler material, improving the particle packing density and reducing the water demand [36]. Furthermore, the use of slag in concrete can improve the durability characteristics, such as resistance to chloride ingress and sulfate attack, due to the refined pore structure and reduced permeability of the concrete matrix [39].

2.6. Silica Fume

It is a silica fume designated by the name "MEDAPLAST HP," a gray powder-based micro silica from the "GRANITEX" company. Its physical characteristics are: absolute density = 1.87, apparent density = 0.5, and specific surface area = 20470 cm2/g.

The absolute density was determined using the pycnometer method, as described in ASTM C188 [31], while the apparent density was measured using the ASTM C29/C29M standard [31]. The specific surface area was determined using the Brunauer–Emmett–Teller (BET) surface area analysis method, as outlined in ASTM C1069 [31].

Silica fume is a highly reactive pozzolanic material that can significantly improve the mechanical properties, durability, and impermeability of concrete when used as a partial replacement for cement [40, 41]. The ultrafine nature of silica fume particles contributes to the enhancement of the interfacial transition zone between the cement paste and aggregate, resulting in a denser and more homogeneous microstructure [42]. The high pozzolanic reactivity of silica fume leads to the formation of additional calcium silicate hydrates, which improve the strength and durability characteristics of the concrete [43].

2.7. Chemical Admixture (Superplasticizer)

The chemical admixture used is the superplasticizer "MEDAFLOW30," produced by the company "GRANITEX." It is in liquid form with light brown color and is based on Polycarboxylates, with a density of 1.07, chlorine content lower than 0.1g*/l,* dry extract of 30%, and pH ranging from 6 to 6.5, according to the manufacturer.

2.8. Mixing Water

The mixing water used complies with the requirements of standard ASTM C1602 [31]. It is potable water from the tap of the public network in the city of Biskra, ensuring the water is free from impurities that could potentially affect the properties of the concrete.

3. Methodology

3.1. Mixes and Formulations

Based on the guidelines provided by [19], several preliminary formulations were conducted to optimize and characterize a 100% cement self-compacting concrete (SCC) that meets the criteria and recommendations for fresh state properties according to [20], with a water-to-cement ratio (W/C) of 0.4 and paste-to-volume ratio (S/paste) of 0.7. Then, a portion of cement was replaced by various mineral additions (30% limestone fillers, 40% blast furnace slag, and 10% silica fume) to obtain four self-compacting concrete mixtures.

The incorporation of mineral additions, such as limestone fillers, blast furnace slag, and silica fume, can significantly enhance the water efficiency of concrete mixtures. These mineral additions contribute to the improvement of water efficiency through different mechanisms. Limestone fillers act as a filler material, improving the particle packing density and reducing the water demand for a given workability [8]. The fine limestone particles can fill the voids between cement and aggregate particles, resulting in a denser and more cohesive mixture.

Blast furnace slag exhibits pozzolanic properties, reacting with calcium hydroxide produced during cement hydration to form additional calcium silicate hydrates [9]. This pozzolanic reaction consumes part of the water, reducing the effective water-to-binder ratio and improving the water efficiency of the mixture. Silica fume, with its ultrafine particle size and high pozzolanic reactivity, can significantly improve the particle packing density and contribute to the formation of additional calcium silicate hydrates [10]. The improved particle packing and pozzolanic reaction led to a reduction in water demand and enhanced water efficiency. By optimizing the combination and proportions of these mineral additions, it is possible to achieve self-compacting concrete mixtures with improved water efficiency, leading to better workability, cohesiveness, and mechanical properties while reducing the water demand and potential for segregation or bleeding [11, 12].

For the vibrated ordinary concrete (VOC), the Dreux-Gorisse method was used in this study [21]. The procedure before studying the adhesion involves two groups of tests. Initially, a self-compacting concrete was formulated and characterized after several preliminary tests, meeting the guidelines of [19] and the fresh state recommendations of AFGC [20]. To determine the mechanical performance of the different concretes, compression behavior characterization tests were carried out in accordance with the norm (NFP 18-406), on cubic specimens with dimensions of (10x10x10 cm^3), cured in water. The compressive strength fcj results at 7,14, 28 and 90 days represent the average of three samples. The testing machine used for uniaxial cube crushing is a hydraulic press with a maximum capacity of 1500 kN in compression. The expression of the results is given by the relation:

$$fcj = \frac{F}{S} \quad (1)$$

Where F is the maximum load and S is the compression surface of the specimen [21]. For flexural tensile tests, tests were conducted on prismatic specimens with dimensions of (10x10x40 cm^3), cured in water, following the norm (NFP 18-406). The tensile strength ft28 obtained at 28 days is the average of results from three samples. The apparatus used is a bending hydraulic press with a maximum capacity of 150 kN in shear. The expression of the results for expressing the flexural tensile strength is given by the relation:

$$ftj = 1.8\frac{F}{a^2} \quad (2)$$

Where F is the rupture load and a is the side of the base in mm. Regarding the elastic modulus at 28 days, it is determined on cylindrical specimens of (16x32 cm^2), cured in water, and equipped with a single-sensor axial extensometer to measure longitudinal deformations of the sample under increasing loads up to a maximum stress equal to:

$$\sigma_c = 0.6 f_{cj} \quad (3)$$

From the equation:

$$\sigma c = Ec\varepsilon c \quad (4)$$

It is possible, according to R. Dupan [22], to plot the curve:

$$\sigma_c = f(\varepsilon_c) \quad (5)$$

For σ ranging from 0 to $0.6f_c$. On this curve, the slope of the tangent at the origin (tangent modulus) and the slope of the line passing through the origin and the coordinate point εc and 0.6fc (secant modulus) can be measured, with:

$$E = 0.6\frac{fc}{\varepsilon c} \quad (6)$$

The evaluation of adhesion between the old and new concrete was conducted through repair simulations. Prismatic specimens with dimensions of 10x10x10 cm^3 and cylindrical specimens with dimensions of 16x32 cm^2 were prepared using ordinary concrete. After 28 days of curing, these specimens were subjected to flexural tensile tests (for prisms) and splitting tensile tests (for cylinders) to obtain half-specimens with exposed aggregates, resulting in rougher surfaces.

Before applying the repair, the rough surfaces of the half-specimens (prismatic and cylindrical) were moistened for 24 hours to achieve the Saturated Surface Dry (SSD) condition. Subsequently, the half-specimens were placed in suitable molds, and the repair concrete (self-compacting concrete, SCC) and the vibrated ordinary concrete (VOC) as a

reference were poured to obtain composite specimens after demolding. The composite specimens consisted of two parts bonded at the interface: the first part formed the base concrete or substrate, and the second part formed the repair concrete or new concrete (Figure 1). This setup allowed for the evaluation of the adhesion between the old (substrate) and new (repair) concrete.

(a) (b)

Fig. 1. The Composite specimens (a) old concrete, (b) repair

Finally, these specimens were kept in water to determine the adhesion between the old and new concrete, we conducted two tests: before being subjected to the crushing tests at the age of 28 days to evaluate the adhesion strength between the old and new concrete.

3.1.1. The First Method (Indirect Tensile Bond Test)

This involves subjecting the composite prismatic specimens to the indirect tensile bond test, which is inspired by the CRD C85 standard. The procedure entails applying a compressive load parallel to the repair interface between the existing concrete and the repair concrete. The bond stress in this method is estimated by the ratio of the load at failure to the surface area, and the whole is adjusted by a correction factor estimated at 0.98.

3.1.2. The Second Method (Splitting Tensile Bond Test)

The cylindrical (composite) specimens are subjected to the splitting tensile bond test to evaluate the quality of adhesion between the old and new concrete. With this method, the bond stress is only that of splitting tensile stress, which will be calculated using the following formula:

$$ftj = 2P/\pi DL \quad (7)$$

Where: P is the maximum compressive load causing the cylinder to split when subjected to tensile stress along the vertical diametral plane; D and L are the diameter and length of the cylinder.

4. Results and Discussion

4.1. Formulation and characterization of fresh SCC

For the formulation of our SCC, we initially focused on optimizing the gravel volume. Five SCC samples with gravel doses ranging from *250 l to 350 l* in increments of 25 *l* were prepared. All mixtures had sand/paste ratios (S/Pt) of 0.6 and water-to-cement ratios

(W/C) of 0.4, along with a superplasticizer content of 0.8%. The results obtained in the fresh state, as shown in Figure 2.a, indicate that increasing the gravel volume considerably reduces the fluidity of the SCC. This reduction can reach 73.68% when the gravel volume increases from 250 *l* to 350 *l*.

This phenomenon is attributed to the insufficient cement paste content due to the increased volume of gravel. In fact, the gravel particles tend to come into contact with each other, leading to increased frictional forces between them, thereby restricting the flow of the SCC. This observation aligns with previous studies on SCC [23, 24]. Similarly, the increase in gravel volume has a negative effect on the filling capacity of the SCC (H2/HI ratio) as shown in Figure 2.b. When the gravel volume reaches 350 *l*, the gravel particles shear and touch, resulting in the formation of clusters against the reinforcements, thus blocking the material. Regarding stability, Figure 2.c shows that the segregation index decreases as the gravel volume increases, even reaching almost zero with a volume of 350 *l*. This decrease is due to the reduction in the volume of cement paste caused by the increased gravel volume, leading to a decrease in the segregation index. Therefore, the increase in gravel volume has a significant impact on the properties in the fresh state and the characterization of the SCC.

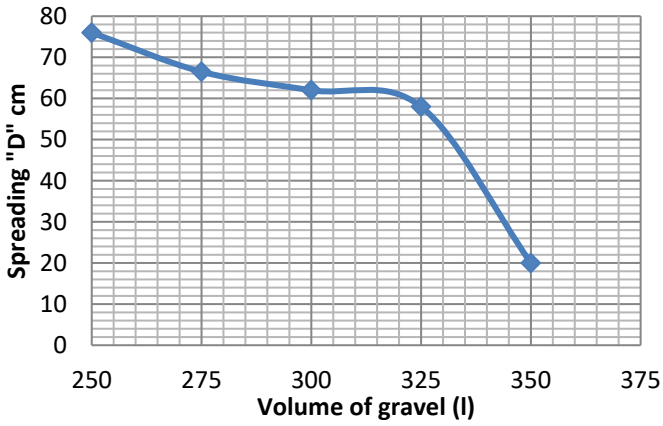

(a)

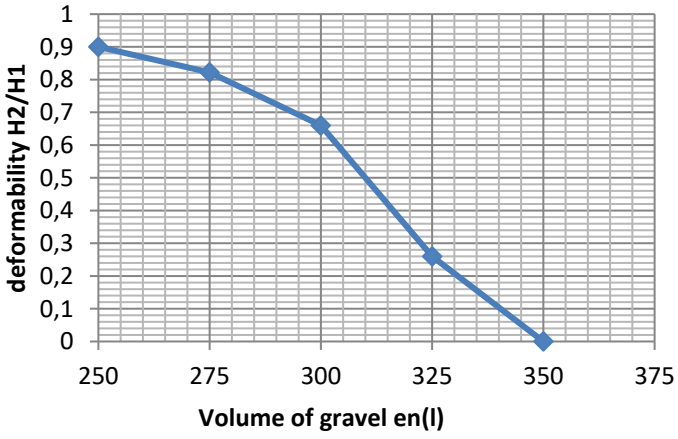

(b)

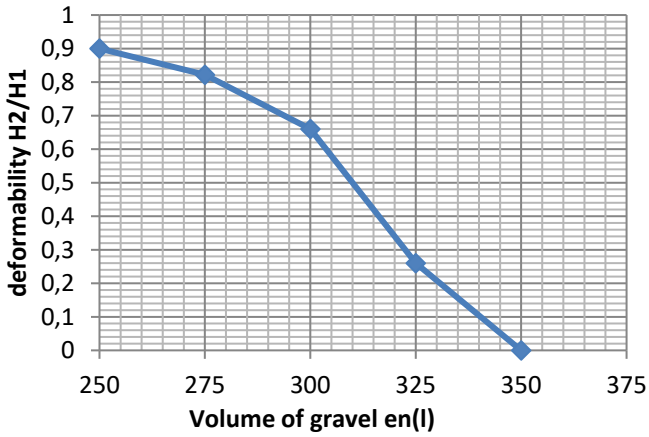

(c)

Fig. 2. Effect of gravel volume on fresh scc properties (a) effect of gravel on fluidity b:effect of gravel deformability, and c: effect of gravel on stability

A gravel dosage of 275 l was identified as the most appropriate to meet the performance criteria while ensuring good adhesion between the mortar and the gravel. To optimize the superplasticizer dosage, nine SCC samples were prepared with a fixed gravel volume of 275 l and W/C ratio of 0.4. The percentages of superplasticizer were varied from 0.8% to 1.2% with an increment of 0.2%, and the S/Pt ratio was varied from 0.6 to 0.8 with an increment of 0.1. The effect of the superplasticizer on the rheological properties is well illustrated in Figure 3 where the increase in spread diameter is directly related to the progressive increase in the superplasticizer dosage. For example, at an S/Pt ratio of 0.6, the spread diameter increases from 66.5 cm to 90 cm when the superplasticizer dosage increases from 0.8% to 1.2% (Figure 3 a). This improvement in fluidity is attributed to the action of long-chain molecules of the superplasticizer, which cause deflocculation of cement particles and lubricate the paste. Additionally, the increase in superplasticizer dosage leads to a higher filling capacity of the mixtures, as shown in Figure 3.b, since deformability is closely linked to fluidity.

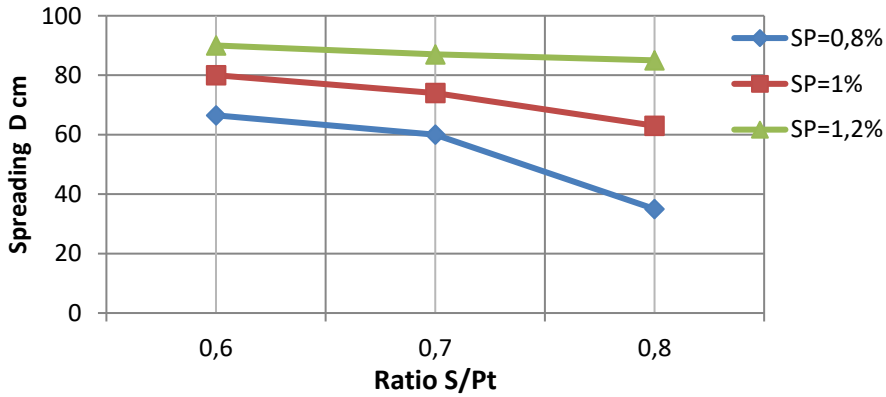

(a)

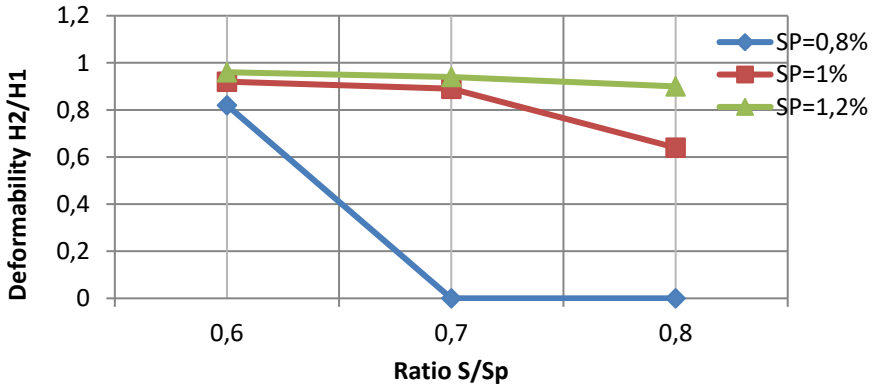

(b)

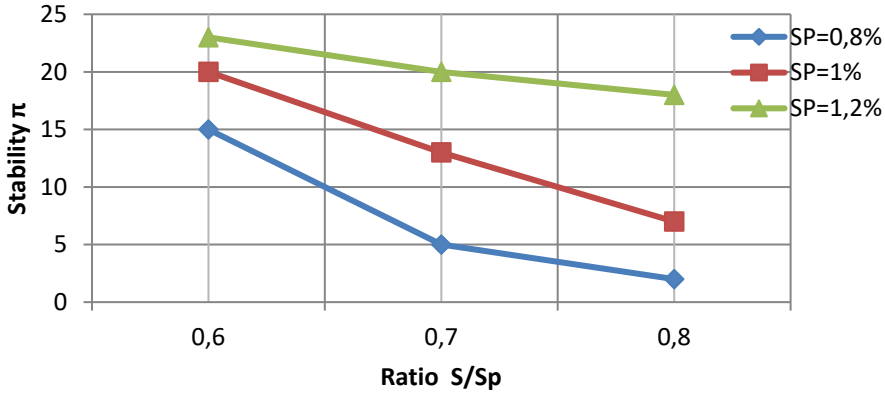

(c)

Fig. 3. Effect of superplasticizer dosage on fresh SCC properties (a) effect of superplasticizer on fluidity, (b) effect of superplasticizer on filling rate (deformability), and (c) effect of superplasticizer on segregation rate (stability)

However, we observed that the increase in superplasticizer dosage also causes a loss of stability, as illustrated in Figure 3.c. The segregation index increases significantly when the superplasticizer dosage goes from 0.8% to 1.2%, which could be problematic for the mechanical properties of the SCC. These results indicate that a dosage of 1% of superplasticizer with an S/Pt ratio of 0.7 provides good fluidity and meets the requirements of self-compacting concrete (SCC). After optimizing the required gravel volume and superplasticizer percentage, the study focused on optimizing the volumetric ratios of S/Pt (sand/paste) and W/C (water/cement) using nine SCC mixtures while keeping the superplasticizer dosage and gravel volume constant. The effect of the S/Pt and W/C ratios on the fluidity of the mixtures is illustrated in Figure 4.

It is observed that for a given W/C ratio, an increase in the S/Pt ratio leads to a decrease in the spread diameter (Figure 4.a). This decrease is attributed to a reduction in the volume of cement paste, which is crucial for ensuring good compatibility of the SCC. Similarly, for all S/Pt ratios, an increase in the W/C ratio improves fluidity, primarily due to the excess water content that reduces internal shear stresses. Regarding the effect of the S/Pt and

W/C ratios on the filling capacity of the mixtures (Figure 4.b), it is observed that the filling rates decrease as the S/Pt ratio increases. To facilitate the passage of SCC through heavily reinforced formwork, the volume of cement paste needs to be adjusted accordingly. This result is consistent with the findings of other researchers [25]. Regarding stability (Figure 4.c), an increase in the S/Pt ratio can reduce the segregation index, while an increase in the W/C ratio can directly influence the segregation rate. An increase in the W/C ratio improves fluidity and deformability but affects stability, whereas an increase in the S/Pt ratio reduces spread diameter and deformability but improves stability. Among all the tested mixtures, only one was considered truly self-compacting, meeting the requirements of the French Association of Civil Engineering (AFGC) [20], with an S/Pt ratio of 0.7, anW/C ratio of 0.4, a superplasticizer dosage of 1%, and a gravel volume of 275 l. These results are in line with those reported in the literature by other researchers [25, 26]. The formulation of SCC with a high cement content can lead to high costs and issues related to heat of hydration. The use of mineral additives can be a solution to improve these properties while reducing the cement quantity. In this study, we analyze the effect of limestone fillers, slag, and silica fume on the workability of SCC. The effect of limestone fillers on the fluidity of SCC is significant (Figure 5.a), with an increase in the spread diameter from 74 cm to 77 cm for a dosage of 30% limestone fillers. This can be explained by the fine nature of limestone fillers, which can fill the gaps between the coarse cement particles and release the trapped water between them.

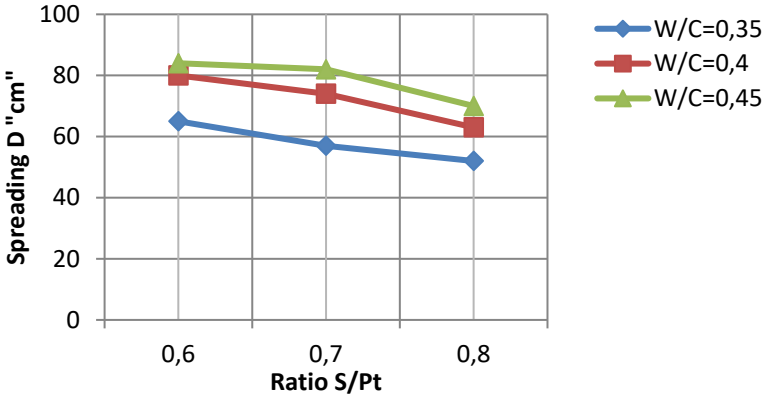

(a)

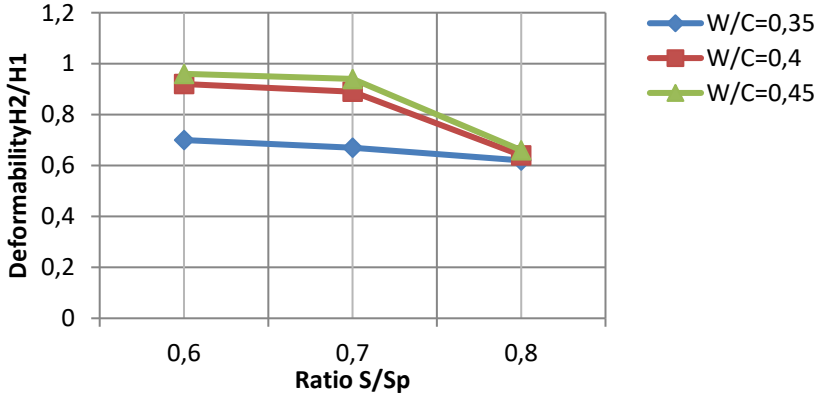

(b)

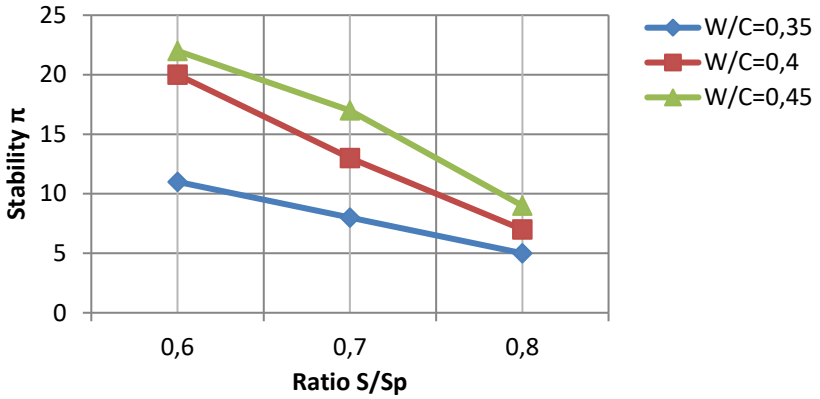

(c)

Fig. 4. Effect of sand/paste ratio (S/P) on fresh SCC properties (a) effect of sand/paste ratio(s/p) on fluidity, (b) effect of sand/paste ratio(s/p) on filling rate (deformability), and (c) effect of sand/paste ratio(s/p) on segregation rate (stability)

On the other hand, slag tends to decrease the spread diameter of SCC, requiring an increase in the dosage of superplasticizer (SP) to maintain its self-placing ability. Silica fume also shows a similar effect, with a decrease in spread diameter and an increased demand for SP to ensure good workability. The deformability of SCC is directly related to its fluidity. Limestone fillers improve deformability, with a filling rate (H2/H1) increasing from 0.89 to 0.95 for a dosage of 30% limestone fillers. For mixtures containing slag or silica fume, an increase in SP dosage is necessary to enhance deformability and achieve a filling rate of 0.78 and 0.82, respectively, as shown in Figure 5.b. Figure 5.c illustrates that the incorporation of limestone fillers and slag improves the stability of SCC, reducing the segregation index from 13% to 10% and 4.5%, respectively.

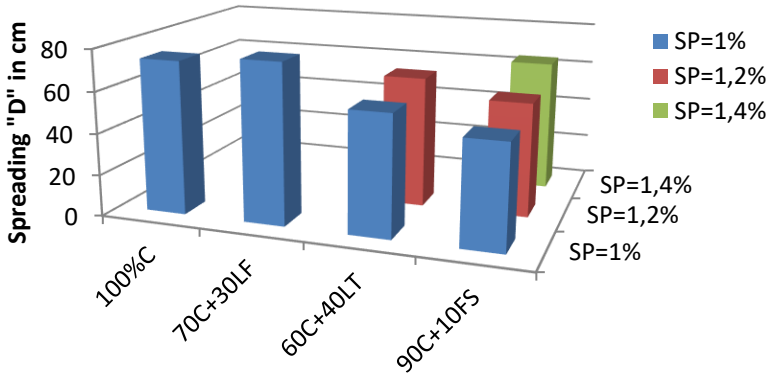

(a)

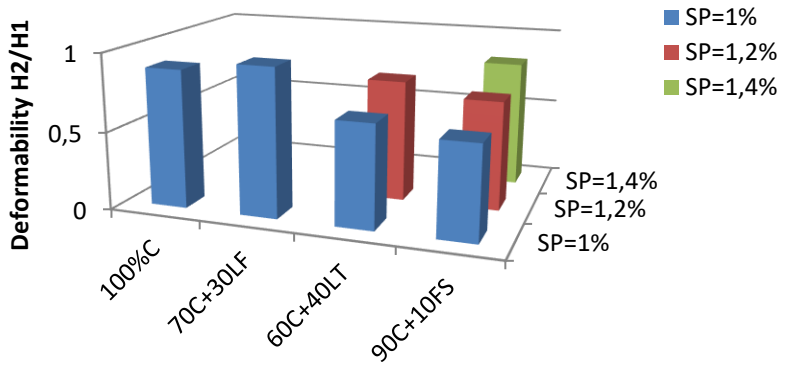

(b)

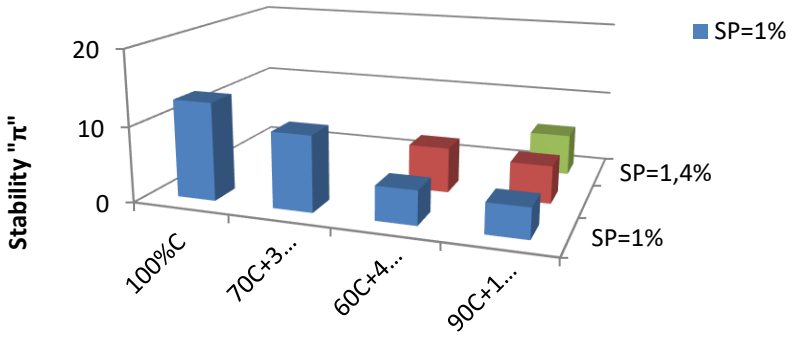

(c)

Fig. 5.Effect of mineral additives on fresh SCC properties (a) effect of mineral additions on fluidity, (b) effect of mineral additions on filling rate (deformability), and (c) effect of mineral additions on segregation rate (stability)

Table 1. presents the compositions of several optimized concrete mixtures, while Table 2 displays the results of fresh state tests conducted on various Self-Compacting Concretes (SCC). Silica fume also exhibits a positive effect on stability, with a segregation rate of only 5.5% for a dosage of 1.4% SP. The use of mineral additives in the formulation of Self-Compacting Concrete (SCC) allows for the improvement of its rheological and mechanical properties.

Table 1. Compositions of various formulated concretes

N°	Designation	Gravel 7/15	Gravel 3/8	Sand	Cement	Addition	Water	SP
		Kg/m³	Kg/m³	Kg/m³	Kg/m³	Kg/m³	l/m³	%
01	SCC100%C	720.5	00	742.67	574.74	00	229.89	1
02	SCC30%LF	720.5	00	742.89	388.75	166.6	222.14	1
03	SCC40%BFS	720.5	00	740.18	335.30	223.53	223.53	1.2
04	SCC10%SF	720.5	00	737.59	501.39	55.71	222.84	1.4
05	VOC	851	261	630	400	00	200	00

Limestone fillers enhance fluidity and deformability, while slag and silica fume improve stability and mechanical strengths. Optimizing the dosage of superplasticizer is essential to maintain the self-placing ability of SCC while benefiting from the advantages of mineral additives.

Table 2. Results of fresh state tests for different self-compacting concretes (SCC)

N°	Designation	Slump flow D in (cm)	Deformability H2/H1	Stability π
01	SCC100%C	74	0.89	13
02	SCC30%LF	77	0.95	10
03	SCC40%BFS	63	0.78	6
04	SCC0%SF	64	0.82	5.5

4.2. Study of Mechanical Properties of Different Optimized Concrete Mixtures in The Hardened State

The evolution of compressive strength at different ages is well illustrated in Figure 6, where we observe that at early ages, all mixtures except those containing slag, develop higher strengths than vibrated ordinary concrete. For example, the 100% cement SCC recorded 32MPa at 14 days, which represents 82% of the strength of ordinary concrete at 28 days (39MPa). Similarly, the 10% silica fume SCC developed a strength of 45MPa at 14 days, representing 115.38% of that of ordinary concrete at 28 days. Concrete mixes based on slag (SCC 40% BFS) exhibit lower strengths at 14 days compared to ordinary concrete, partly because slag does not have enough time at 14 days to contribute to strength development, and also due to the lower cement content in slag-based concrete. At long term (90 days), it is observed that all self-compacting concretes, regardless of the substitution type, recorded higher strengths than ordinary concrete. For instance, the 100% cement SCC showed a strength of 58MPa compared to 47MPa for ordinary concrete, the SCC30% LF developed a strength of 46MPa, and the SCC10%SF marked a strength of 70MPa. Similarly, the slag-based SCC (40%) at long term showed a strength of 52MPa, surpassing the 47MPa of ordinary concrete at 90 days due to its pozzolanic property. Regarding the evolution of tensile strength, according to Figure 7, all SCCs developed slightly higher tensile strengths at the age of 28 days compared to ordinary concrete.

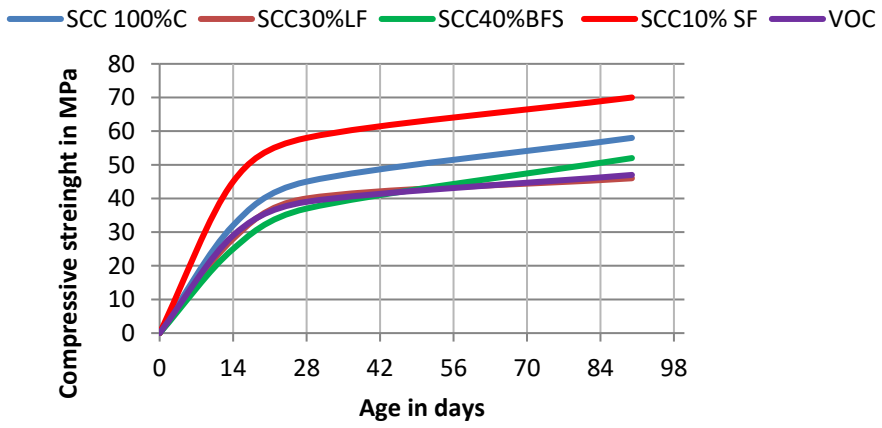

Fig. 6. Evolution of compressive strength over

Specifically, the SCC100% cement showed a tensile strength of 3.3MPa, the SCC30% LF 3MPa, and the SCC10%SF 4.2MPa, while vibrate ordinary concrete had a tensile strength of 3MPa. However, the SCC 40% BFS recorded a tensile strength of 2.9MPa, which can be attributed to the fact that the 40% substitution is at its maximum, and at 28 days, this mixture containing slag has not yet developed its mechanical properties. The highest result was obtained for the SCC10% BFS (4.2MPa), indicating the homogeneity and proper distribution of aggregates in the binder paste.

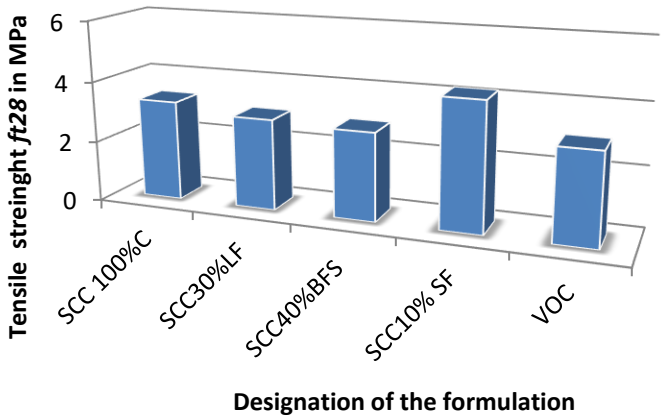

Fig.7. Tensile strength at 28 days of different concretes

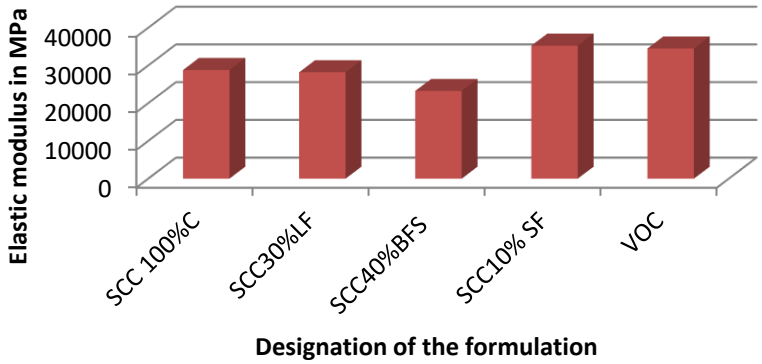

Fig. 8. Elastic modulus at 28 days of different concretes

This homogeneity is ensured by the presence of the superplasticizer, which disperses the cement grain stacking and silica fume particles. Regarding the elastic modulus, which is generally affected by the gravel content, SCCs are likely to be more deformable than ordinary concrete. As shown in Figure 8, the elastic modulus of SCC is consistently lower than that of ordinary concrete. For example, at 28 days, the elastic modulus is 28800MPa for 100% cement SCC, 28200MPa for SCC 30% LF, 23250MPa for SCC40%BFS and 34500MPa for vibrated ordinary concrete. These results are confirmed by AFGC and have also been found by several researchers [4], [24] and [27]. On the other hand, the SCC10%SF

yielded an elastic modulus of 35250MPa, higher than that of ordinary concrete, which can be attributed to its higher compressive strength as well.

4.3. Evaluation of The Bond Strength Between Old and New Concrete

The first observation we made during the evaluation of bond strength is that the test on prismatic specimens yields higher results compared to the splitting tensile test on cylindrical specimens. As shown in Figure 9, the bond strength for 100% cement SCC is 2.64MPa for the test on prisms, compared to 1.92 MPa on cylinders. Similarly, the 30% LF SCC recorded 1.96MPa on prisms and 1.74MPa on cylinders, and the SCC40% BFS showed 1.52MPa on prisms and 1.36MPa on cylinders.

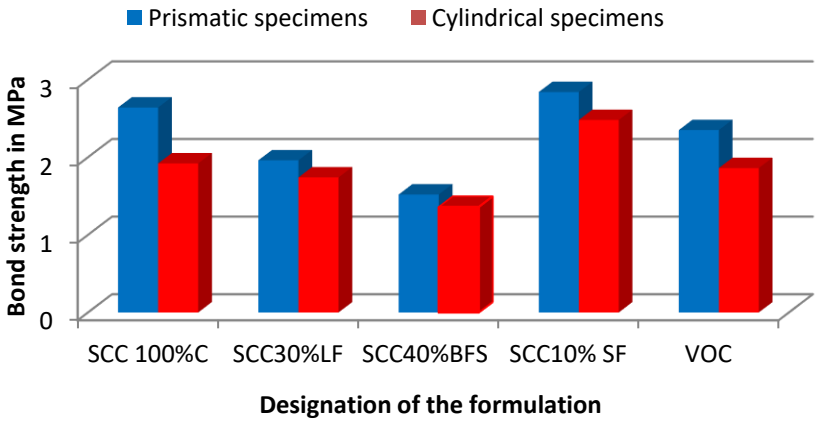

Fig. 9. Bond strength for different repair mixes

The second observation is that the bond strengths of all SCCs generally follow the trend of tensile strength. It can be noted that the 10% FS mixture offers the best bond strength in both the prism and cylindrical tests (2.84MPa and 2.48MPa) compared to 2.35MPa and 1.86MPa for ordinary concrete, respectively. This result is confirmed by Soneibi [25]. The lowest result compared to ordinary concrete was found for the SCC30% LF with 1.96 MPa on prisms and 1.74 MPa on cylinders, but it was even lower for the SCC40%BFS with 1.52MPa on prisms and 1.36MPa on cylinders. This can be attributed to the low cement content in this mixture (335.5kg/m^3) and the low specific surface area of the slag used (3070cm^2/g).

5. Conclusion

This comprehensive study evaluated the potential of utilizing Self-Compacting Concrete (SCC) as an effective repair material for concrete structures. Through a systematic approach, various SCC mixtures were formulated with different compositions, including 100% cement, 30% limestone fillers, 40% blast furnace slag, and 10% silica fume. The primary objective was to optimize the fresh properties, such as fluidity, deformability, and stability, to ensure compliance with the requirements for self-compacting concrete in repair applications.

The mechanical properties of the optimized SCC mixtures were extensively characterized and compared to those of vibrated ordinary concrete (VOC). Remarkably, all SCC mixtures exhibited higher compressive strengths than VOC at later ages, with the 10% silica fume SCC outperforming the others by achieving the highest compressive strength. This

superior performance can be attributed to the pozzolanic activity of silica fume, which contributed to the formation of additional calcium silicate hydrates, resulting in a denser and stronger concrete matrix. Furthermore, the tensile strengths of the SCC mixtures were evaluated at 28 days, and all mixtures demonstrated slightly higher values compared to VOC. Once again, the 10% silica fume SCC emerged as the top performer, exhibiting the highest tensile strength among all mixtures. This can be attributed to the improved interfacial transition zone between the cement paste and aggregates, as well as the homogeneous distribution of silica fume particles within the concrete matrix.

A crucial aspect of this study was the assessment of the bond strength between the SCC repair material and the existing concrete substrate. Simulated repair specimens were subjected to indirect tensile bond and splitting tensile bond tests to quantify the adhesion between the old and new concrete interfaces. The results revealed that the SCC mixtures generally exhibited higher bond strengths compared to VOC, with the 10% silica fume SCC demonstrating the best bond strength performance. This superior adhesion can be attributed to the improved microstructure and reduced porosity of the SCC mixtures, leading to enhanced mechanical interlocking and chemical bonding mechanisms at the repair interface. The incorporation of mineral additives, such as limestone fillers, blast furnace slag, and silica fume, played a pivotal role in influencing the fresh and hardened properties of the SCC mixtures. Limestone fillers contributed to improved fluidity, deformability, and stability by enhancing the particle packing density and reducing the water demand. On the other hand, blast furnace slag and silica fume exhibited positive effects on mechanical strengths and bond strength, albeit with a slight reduction in workability due to their higher water demand.

Overall, this study highlights the promising potential of using SCC as a superior repair material for concrete structures. The superior mechanical performance, enhanced bond strength, and the ability to incorporate mineral additives make SCC an attractive choice for concrete repair applications. The improved durability and longevity offered by SCC can lead to more sustainable and cost-effective repair solutions, ultimately extending the service life of concrete structures and reducing the need for frequent repairs or replacements.

References

[1] Srinath D, Ramesh G, Ramya D, Krishna BV. WITHDRAWN: Mechanical properties of sustainable concrete by using RHA and hydrated lime. 2021. https://doi.org/10.1016/j.matpr.2021.02.785

[2] Bissonnette B. Le fluage en traction: un aspect important de la problematique des reparations minces en beton. Université Laval; 1997.

[3] Billel R. Contribution to study the effect of (Reuss, LRVE, Tamura) models on the axial and shear stress of sandwich FGM plate (Ti-6A1-4V/ZrO2) subjected on linear and nonlinear thermal loads. AIMS Materials Science. 2023;10(1). https://www.aimspress.com/article/doi/10.3934/matersci.2023002

[4] Molez L. Comportement des réparations structurales en béton: couplage des effets hydriques et mécaniques [Doctoral dissertation]. École normale supérieure de Cachan-ENS Cachan; Université Laval; 2003.

[5] Courard L, Bissonnette B. Essai dérivé de l'essai d'adhérence pour la caractérisation de la cohésion superficielle des supports en béton dans les travaux de réparation: analyse des paramètres d'essai. Materials and Structures. 2004;37(269). https://hdl.handle.net/2268/17594

[6] Bissonnette B, Courard L, Jolin M, Thomassin M, Vaysburd A, Garbacz A, von Fay K. Adhérence des réparations en béton: évaluation et facteurs d'influence. In: Journées scientifiques du (RF)B. 2014. https://hdl.handle.net/2268/171851

[7] Bissonnette B, Vaysburd AM, von Fay KF. Best practices for preparing concrete surfaces prior to repairs and overlays. No. MERL 12-17. 2012. http://www.usbr.gov/research/projects/download_product.cfm?id=446
[8] Morgan DR. Compatibility of concrete repair materials and systems. Construction and building materials. 1996;10(1):57-67. https://doi.org/10.1016/0950-0618(95)00060-7
[9] Luković M, Ye G, Van Breugel K. Reliable concrete repair-a critical review. In: Proc. of international conference Structural Faults & Repair; 2012.
[10] Jumaat MZ, Kabir MH, Obaydullah M. A review of the repair of reinforced concrete beams. Journal of Applied Science Research. 2006;2(6):317-326. http://eprints.um.edu.my/id/eprint/6103
[11] Manawadu A, Qiao P, Wen H. Characterization of substrate-to-overlay interface bond in concrete repairs: a review. Construction and Building Materials. 2023;373:130828. https://doi.org/10.1016/j.conbuildmat.2023.130828
[12] Page CL, Ngala VT, Page MM. Corrosion inhibitors in concrete repair systems. Magazine of Concrete Research. 2000;52(1):25-37. https://doi.org/10.1680/macr.2000.52.1.25
[13] Kuhlmann LA. Test method for measuring the bond strength of latex-modified concrete and mortar. Materials Journal. 1990;87(4):387-394.
[14] Espeche AD, León J. Estimation of bond strength envelopes for old-to-new concrete interfaces based on a cylinder splitting test. Construction and building materials. 2011;25(3):1222-1235. https://doi.org/10.1016/j.conbuildmat.2010.09.032
[15] Le HT, Müller M, Siewert K, Ludwig H-M. The mix design for self-compacting high performance concrete containing various mineral admixtures. Materials and Design. 2015;72:51-62. https://doi.org/10.1016/j.matdes.2015.01.006
[16] Belmokretar K, Ayed K, Kerdal DE, Leklou N, Mouli M. New Repair Material for Ordinary Concrete Substrates: Investigating Self-Compacting Sand Concrete and Its Interaction with Roughness of the Substrate Surface. Journal of Materials in Civil Engineering. 2023;35(9):05023004. https://doi.org/10.1061/JMCEE7.MTENG-15348
[17] Arasteh Khoshbin O, Madandoust R, Ranjbar MM. Evaluation of pull-off strength for steel fibre reinforced self-compacting concrete repair overlays. European Journal of Environmental and Civil Engineering. 2023;27(16):4613-4628. https://doi.org/10.1080/19648189.2023.2194953
[18] Setiawan ES, Sriwahyuni Y, Kartika N. Analisis Efektivitas Kemampuan Pulih Mandiri Micro Crack pada Self-Healing Concrete. Rekayasa Sipil. 2023;17(2):169-178. https://doi.org/10.21776/ub.rekayasasipil.2023.017.02.8
[19] Pandey S, Umale S, More S, Kale NK. Study of the Long-Term Durability of Self-Healing Concrete. International Journal of Advanced Research in Science, Communication and Technology. 2023.
[20] EFNARC. Specifications and Guidelines for the use of specialist products for Mechanized Tunnelling (TBM) in Soft Ground and Hard Rock. Recommendation of European federation of producers and contractors of specialist products for structures; 2005.
[21] Association française de génie civil. Recommandations pour l'emploi des bétons auto-plaçants: recommendations for use of self-compacting concrete. AFGC; 2008.
[22] Ramesh G, Srinath D, Ramya D, Krishna BV. WITHDRAWN: Repair, rehabilitation and retrofitting of reinforced concrete structures by using non-destructive testing methods. 2021. https://doi.org/10.1016/j.matpr.2021.02.778
[23] Adhikary SK, Ashish DK, Sharma H, Patel J, Rudžionis Ž, Al-Ajamee M, et al. Lightweight self-compacting concrete: A review. Resources, Conservation & Recycling Advances. 2022;15:200107. https://doi.org/10.1016/j.rcradv.2022.200107

[24] Rahman SK, Al-Ameri R. Marine Geopolymer Concrete—A Hybrid Curable Self-Compacting Sustainable Concrete for Marine Applications. Applied Sciences. 2022;12(6):3116. https://doi.org/10.3390/app12063116
[25] Ramesh G. Self-Compacting Concrete: A Review. Indian Journal of Structure Engineering (IJSE). 2021;1(2):9-12. https://www.ijse.latticescipub.com/portfolio-item/a1303051121/
[26] Rajendrana D, Christopher CG, Muthu MS. Self-compacting concrete made with partial replacement of lime stone and quarry dust powder. Res. Eng. Struct. Mater. 2022;8:633-642. http://dx.doi.org/10.17515/resm2022.346ma1001tn
[27] Alghamri R, Rengaraju S, Al-Tabbaa A. Large-scale laboratory trials of smart aggregates for self-healing in concrete under different curing regimes. Cement and Concrete Composites. 2023;136:104864. https://doi.org/10.1016/j.cemconcomp.2022.104864
[28] Nécira B, Abadou Y. Properties of self-compacting mortar made with various mineralogical sources different types of sands and fillers. World Journal of Engineering. 2021;18(6):861-869. https://doi.org/10.1108/WJE-10-2020-0483
[29] Memiş S. Performance Characteristics and Cost Optimization of Self-Compacting Concrete with Industrial Waste Additives to be Used in Agricultural Buildings. Turkish Journal of Agriculture-Food Science and Technology. 2021;9(1):89-97. https://doi.org/10.24925/turjaf.v9i1.89-97.3731
[30] De Larrard F. Concrete mixture proportioning: a scientific approach. CRC Press; 1999.
[31] ASTM International. ASTM C131/C131M - Standard Test Method for Resistance to Degradation of Small-Size Coarse Aggregate by Abrasion and Impact in the Los Angeles Machine. West Conshohocken, PA; 2020.
[32] Okamura H, Ouchi M. Self-compacting concrete. Journal of advanced concrete technology. 2003;1(1):5-15. https://doi.org/10.3151/jact.1.5
[33] Neville AM, Brooks JJ. Concrete Technology. 2nd ed. Pearson Education Limited; 2010.
[34] Mehta PK, Monteiro PJM. Concrete: Microstructure, Properties, and Materials. 4th ed. McGraw-Hill Education; 2014.
[35] Uysal M, Yilmaz K. Effect of mineral admixtures on properties of self-compacting concrete. Cement and Concrete composites. 2011;33(7):771-776. https://doi.org/10.1016/j.cemconcomp.2011.04.005
[36] Ghezal A, Khayat KH. Optimizing self-consolidating concrete with limestone filler by using statistical factorial design methods. Materials Journal. 2002;99(3):264-272. https://www.concrete.org/publications/acimaterialsjournal.aspx
[37] Ye G, Liu X, De Schutter G, Poppe AM, Taerwe L. Influence of limestone powder used as filler in SCC on hydration and microstructure of cement pastes. Cement and Concrete Composites. 2007;29(2):94-102. https://doi.org/10.1016/j.cemconcomp.2006.09.003
[38] Oner AD, Akyuz S. An experimental study on optimum usage of GGBS for the compressive strength of concrete. Cement and concrete composites. 2007;29(6):505-514. https://doi.org/10.1016/j.cemconcomp.2007.01.001
[39] Kou SC, Poon CS. Properties of self-compacting concrete prepared with recycled glass aggregate. Cement and Concrete Composites. 2009;31(2):107-113. https://doi.org/10.1016/j.cemconcomp.2008.12.002
[40] Bache HH. Densified cement ultra-fine particle-based materials; 1981.
[41] Neville AM. Properties of concrete. Vol. 4. London: Longman; 1995.
[42] Goldman A, Bentur A. The influence of microfillers on enhancement of concrete strength. Cement and concrete research. 1993;23(4):962-972. https://doi.org/10.1016/0008-8846(93)90050-I
[43] Mouli M, Khelafi H. Performance characteristics of lightweight aggregate concrete containing natural pozzolan. Building and environment. 2008;43(1):31-36. https://doi.org/10.1016/j.buildenv.2006.11.038